Theory of ground-state switching in an array of magnetic nanodots by application of a short external magnetic field pulse

Roman Verba,[1] Vasil Tiberkevich,[2] Konstantin Guslienko,[3,4] Gennadiy Melkov,[1] and Andrei Slavin[2]
[1]*Faculty of Radiophysics, Taras Shevchenko National University of Kyiv, Kyiv 01601, Ukraine*
[2]*Department of Physics, Oakland University, Rochester, Michigan 48309, USA*
[3]*Departamento de Fisica de Materiales, Universidad del Pais Vasco, 20018 San Sebastián, Spain*
[4]*IKERBASQUE, The Basque Foundation for Science, 48011 Bilbao, Spain*
(Received 20 February 2013; revised manuscript received 1 April 2013; published 22 April 2013)

A theory of a ground-state switching in an array of axially magnetized cylindrical magnetic dots arranged in a square lattice is developed. An array can be switched into a quasiregular chessboard-antiferromagnetic state by the application of a short pulse of external in-plane magnetic field having a sufficiently long trailing front. The statistical properties of an array magnetization in its final (after switching) state are determined at the linear stage of growth of unstable collective spin-wave modes of the array under the action of a time-dependent magnetic field, and depend critically on the rate of the field decrease: the slower this decrease, the more regular is the final magnetization state. An analytical procedure is presented that allows one to relate the statistical properties of the final demagnetized state of the array and the linewidth of the array's microwave absorption to the parameters of the external switching pulse. The comparison of the developed analytic theory with the results of numerical simulations is presented and demonstrates good agreement between analytical and numerical results.

DOI: 10.1103/PhysRevB.87.134419 PACS number(s): 75.75.−c, 75.78.−n, 75.30.Ds

I. INTRODUCTION

The magnetic structures with periodic variations of magnetic parameters [magnonic crystals (MCs)] have been attracting much attention recently due to their possible applications in microwave technology and signal processing.[1] All the MCs can be classified into two main types. The MCs of the first type are formed from continuous magnetic materials by periodic modulation of the material parameters, for instance, by variation of a ferromagnetic film thickness,[2,3] formation of an antidot lattice,[4,5] or application of a periodic external magnetic field.[6] These periodic variations of the magnetic parameters lead to significant changes in spin-wave (SW) spectrum of the periodically modulated medium, and, in particular, to the formation of prohibited frequency bands (or stop bands). In has been shown recently[6] that the position and the depth of these stop bands in a periodically modulated medium can be controlled dynamically.

The MCs of the second type are formed by periodic arrays of distinct magnetic elements (e.g., magnetic nanowires[7] or nanodots[8]), usually coupled by the long-range magnetodipolar interaction. The main characteristic feature of this second type of MCs is their multistability, i.e., existence in them of many different ground states (static magnetization configuration). It should be noted that at the zero external field, the ground state of an individual magnetic element is at least double degenerate since the magnetic energy is an even function of the magnetization. Therefore, there are many possible static magnetic configurations in an array of magnetic elements under the same external conditions. The magnetodipolar interaction between the elements removes the degeneracy of different magnetization configurations of the MC leading to the instability of most of them.

Nevertheless, there is a large region of the array's parameters in which an array could have several stable ground states, separated by energy barriers.[9–11] Different ground states correspond to different SW spectra and, as a consequence, to different microwave properties of an array, which has been demonstrated both theoretically[11,12] and experimentally.[13,14] Also, in contrast with the conventional magnetic materials, the multistable magnetic materials with tunable properties could be used without the application of a permanent bias magnetic field.

It is of a great practical interest to find simple methods of ground-state switching in a MC based on an array of individual magnetic elements. In principle, every dot in an array can be switched independently, for example, by means of spin-transfer torque effect.[15] However, the arrangement in which each individual dot in an array is addressed independently will greatly complicate the fabrication of an MC and will substantially increase the MC cost.

One of the ways to switch a ground state of an array of magnetic elements without addressing each individual element is to fabricate an array consisting of several groups of magnetic elements with different geometry. Since the elements in each group have different reversal fields, by applying external magnetic fields of different magnitude, one can reverse the magnetization direction in each separate group of elements, thus achieving different ground states of the array. This concept was successfully realized experimentally with an array of magnetic stripes having different width.[13,14]

This method, however, has several drawbacks. First of all, the structure of the SW spectrum in arrays consisting of several groups of elements is rather complex, as the number of the SW branches in such a composite array can not be smaller than the number of magnetic sublattices, which, in its turn, is no less than the number of different groups of elements in the array.[12]

Thus, even in the case when all the array elements are ferromagnetically ordered (magnetized in the same direction), the spectrum of a ferromagnetic resonance (FMR) in such a composite array consists of several absorption peaks. Also, the process of switching between different ground states in

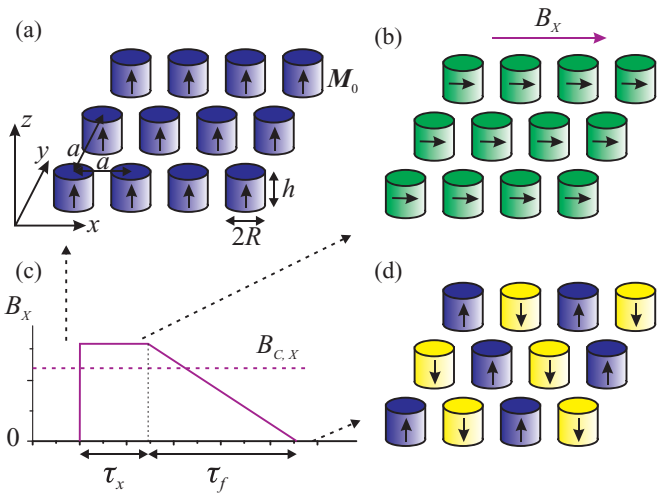

FIG. 1. (Color online) Scheme of the ground-state switching in an array of dipolarly coupled magnetic dots: (a) initial out-of-plane ferromagnetic (FM) ground state; (b) transient in-plane FM state reached after the application of an in-plane magnetic field pulse with magnitude greater than a certain critical value $B_{c,x}$; (c) temporal profile of the switching in-plane magnetic field pulse; (d) final chessboard-antiferromagnetic (CAFM) ground state reached after the end of the switching pulse.

a composite array is quasistatic and, therefore, rather slow, requiring times of the order of a second for each ground-state switching.[13]

In our previous work (Ref. 16), we proposed a method of ground-state switching in an array consisting of identical single-domain perpendicularly magnetized cylindrical magnetic nanodots, arranged in a square lattice. The two simplest stable ground states of such an array at zero external bias magnetic field are the ferromagnetic (FM) and chessboard-antiferromagnetic (CAFM, see Fig. 1) states. The prominent feature of such an array is the degeneracy of the SW branches in the CAFM state at zero wave vector,[11,12] leading to only one peak in its microwave absorption spectrum.

While switching of the array of identical elements into a FM state is trivial (one just needs to apply a field pulse of a sufficiently large amplitude in the direction of the static magnetization of dots), the switching into a CAFM state is not so simple. By means of numerical simulations we have shown in Ref. 16 that after the application of an in-plane bias field pulse with long trailing front, the array switches into a state consisting of clusters with CAFM periodicity. The sizes of these clusters and, therefore, the microwave properties of the array after the switching, depend on the length of the trailing front of the applied bias field pulse (see Sec. II). The typical time range of switching is of the order of 100 ns.

Our present work is devoted to the theoretical consideration of the switching process in an array of dipolarly coupled identical magnetic dots. The main goal of this work is to find relations between the parameters of the externally applied bias magnetic field pulse and the properties of the final (after switching) magnetization state of the dot array. Although most of the equations presented in the text were obtained for an array of axially magnetized cylindrical magnetic dots arranged in a square lattice [Fig. 1(a)], the developed theory of the array switching is general, and can be applied to any array switched into a regular demagnetized state. Following, we discuss what changes in the final expressions are necessary to make them applicable for a different array geometry or/and the different magnetization direction.

We note that the problem of the magnetization relaxation in arrays of dipolarly coupled magnetic elements with perpendicular anisotropy has been previously discussed in literature.[17–19] Also, the processes of spin lattice ordering under the action of thermal fluctuations have been discussed in Refs. 20 and 21. The principal difference between these previously published results and our current work is in the fact that previously the relaxation of the magnetization state was considered as a sequence of thermally activated random jumps of magnetic moments (from the orientation $M_z = \pm M_s$ to the opposite), while in our current work, the magnetization relaxation to a final state on a short-time scale is mostly determined by a different process: the growth of the spin-wave instability.

The paper is organized as follows. In Sec. II, we describe the method of a ground-state switching in an array of dipolarly coupled magnetic dots and the main features of the switching process observed in numerical simulations. The magnetization dynamics of the switching process and the statistical properties of a final state of the array are considered in Sec. III. Then, we compare the predictions of the analytic theory with the results of numerical simulations (Sec. IV) and consider microwave properties of the array in its final state (Sec. V). Finally, a summary of the obtained results and conclusions are presented in Sec. VI.

II. METHOD OF GROUND-STATE SWITCHING

As it was mentioned above, a magnonic crystal in the form of an array of dipolarly coupled magnetic elements in the absence of an external bias magnetic field may have more than one stable ground state and these states may have distinctly different microwave absorption properties. For a square array of magnetic dots with radius R and height h with out-of-plane shape anisotropy ($h/R \gtrsim 2$, see Ref. 22), one of such possible states is the out-of-plane FM state, when all the dots are magnetized in the same out-of-plane direction [see Fig. 1(a)]. Another possible state (and this is the*true ground state* of the array corresponding to the *absolute minimum of its energy*) is the CAFM state, in which magnetizations of neighboring dots are opposite [Fig. 1(d)]. Obviously, any array of magnetic dots under the influence of thermal fluctuations tends ro reach its true ground state (CAFM for our particular geometry), but such thermal relaxation is useless for applications as it requires a very long time (typically in a range of minutes, hours, and more) or a significant heating of an array which can destroy it.

Another and more practical way to make an array of dots to relax into its true ground state is to put an array into a *uniform but unstable* state by application of an external field pulse. In the following, we will call such an unstable state existing only during the application of a switching magnetic field pulse a *transient* state. After removal of the switching pulse, the array will relax from the transient state into the most probable state, which is expected to be close to the ideal CAFM ground state. Obviously, the magnetizations of dots in the transient state, which is, in fact, an in-plane FM state

[see Fig. 1(b)], have to be perpendicular to magnetizations of the dots in a true ground CAFM state. This unstable transient state is realized under the action of an in-plane magnetic field with the magnitude $B_x > B_{c,x}$, where the critical field B_c is equal to

$$B_{c,x} = \mu_0 M_s \left(F_{\mathbf{0}}^{xx} - F_{\boldsymbol{\kappa}}^{zz}\right). \tag{2.1}$$

Here, $\hat{\boldsymbol{F}}_{\boldsymbol{k}}$ is the array's demagnetization tensor, defined in Ref. 12, μ_0 is the vacuum permeability, M_s is the saturation magnetization, and $\boldsymbol{\kappa} = \pi \boldsymbol{e}_x/a + \pi \boldsymbol{e}_y/a$, where a is the lattice constant, is the wave vector corresponding to the minimum in the spin wave spectrum of the dot array in the in-plane FM state. If duration τ_x of a pulse with amplitude B_x [see Fig. 1(c)] exceeds the critical value $\tau_x > \tau_{c,x}$, where

$$\tau_{c,x} \sim \frac{\ln[(B_x - B_{c,x}) M_s V / k_B T]}{2\gamma (B_x - B_{c,x}) \alpha_G}, \tag{2.2}$$

an array reaches a state of thermal equilibrium at the in-plane field B_x and temperature T, and, therefore, loses all the memory about its previous state. In the equation above, V is the volume of a dot, k_B is the Boltzmann constant, γ is the gyromagnetic ratio, and α_G is the Gilbert damping constant of the dot magnetic material.

On the other hand, if the external in-plane bias magnetic field, which created the transient state, decreases below the critical value $B_{c,x}$, the transient state becomes unstable, and the array starts to switch into another state. The most probable final state is the CAFM state since even at a nonzero in-plane field $B_e < B_{c,x}$ the energy minimum corresponds to the arrangement of z component of the dots' magnetization into a CAFM periodicity. However, the CAFM state is double degenerate: two different, but equivalent, configurations are related by the inversion of the magnetization of all dots. Obviously, due to this degeneracy and thermal fluctuations, the whole array can not reach the ideal periodic true CAFM ground state. Instead, the array is separated into clusters with local ideal periodicity of two different degenerate kinds. The sizes of clusters of two degenerate CAFM states depend significantly not only on the array geometry, but also on the time rate of decrease of the in-plane bias magnetic field[16] [i.e., on the duration of pulse trailing front τ_f; see Fig. 1(c)]. When the bias field decreases at a slower rate, the size of clusters becomes larger (see examples in Fig. 2). In a real-life situation, with arrays consisting of millions of dots, it would be practically impossible to achieve the ideal CAFM state, and the remanent state will always contain many CAFM clusters. However, concerning the microwave properties of an array in the resulting CAFM state and, in particular, the absorption spectrum of an array, the case of an array divided into large CAFM clusters (with hundreds of dots in each cluster) is practically indistinguishable from the case of an ideal CAFM array. Thus, for microwave applications, the existence of several large CAFM clusters in the final state of an array is not important.

It should be noted that in all the above-presented calculations, as well as in the further considerations, we use the macrospin approximation, thus, assuming the uniform magnetization distribution inside a dot during the whole switching process. In other words, we use the classical Stoner-Wohlfarth model[23] for the dot magnetization reversal. This model is correct for sufficiently small magnetic nanodots, having radius $R < 3.5 l_{ex}$ [l_{ex} is the exchange length (for permalloy $l_{ex} \approx 5.5$ nm)]. The last condition is satisfied for the dots made from soft magnetic materials in a single-domain state at remanence.[24] However, the assumption of the uniform dot magnetization during the *whole* switching process is not crucial for the remagnetization theory developed in this paper. As it will be explained in the following, the only critical requirement for the theory is the assumption that a soft spin-wave mode inside the magnetic dot has a quasiuniform magnetization profile in the transient state of the array.

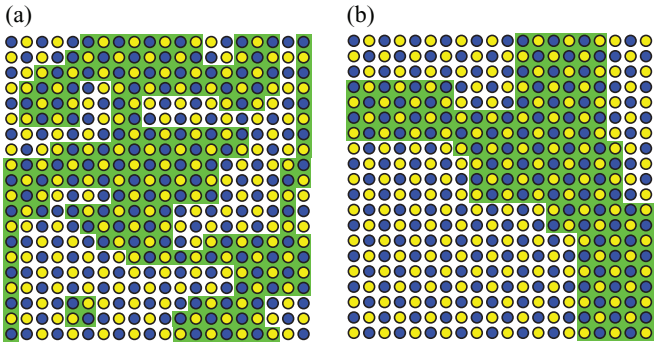

FIG. 2. (Color online) Examples of final states in a magnetic dot array reached after the application of an in-plane magnetic field pulse with different durations of the trailing front: (a) $\tau_f = 2000/\omega_M$; (b) $\tau_f = 6000/\omega_M$, where $\omega_M = \gamma \mu_0 M_s$. Blue (dark gray) and yellow (light gray) circles correspond to the dots having the magnetization directed up and down, respectively. Green (gray) background indicates clusters with the CAFM periodicity $\mu_j = (-1)^{j_x + j_y}$, while the rest of the dots form clusters with inverse periodicity $\mu_j = -(-1)^{j_x + j_y}$ (indices j_x and j_y denote position of a dot in an array).

III. THEORY OF SWITCHING

In this section, we present a theoretical description of the switching process of an array of magnetic dots into a final demagnetized state. First, we formulate a model of magnetization dynamics while switching. Then, we develop a convenient way to describe the properties of the final state of the array. After this, we derive dynamical equations for the dots' magnetizations, solve them, and find the statistical properties of a final state of the dot array. Finally, we formulate the limits of applicability of the developed theory.

A. Model of switching

In the following, we will denote the position of the bottom of the array's SW spectrum in the transient state as $\boldsymbol{\kappa}$. For the square array considered in this calculation, this is the "M" point of the first Brillouin zone (1BZ) $\boldsymbol{\kappa} = \pi \boldsymbol{e}_x/a + \pi \boldsymbol{e}_y/a$ (see Fig. 3). Note that, in principle, there could be more than one bottom points in the SW spectrum of the array within the first Brillouin zone, and, thus, several wave vectors $\boldsymbol{\kappa}_i$, so-called "star" wave vectors. It may seem that for a square array considered here there are four points of spectrum minimum located in the corners of the 1BZ. However, all these points are physically equivalent, and by the shift of the 1BZ one can obtain a Brillouin zone with only one value of $\boldsymbol{\kappa}$. All the theory developed in the following is also valid in such a case. Also

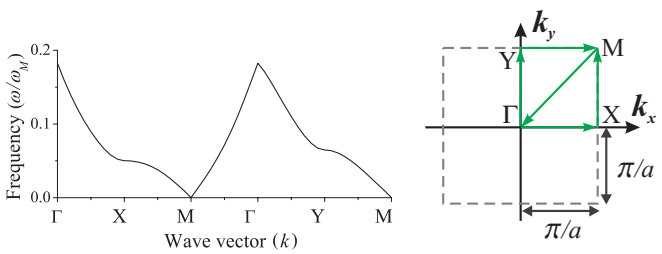

FIG. 3. (Color online) (a) Spin-wave (SW) spectrum of a square array of dipolarly coupled cylindrical nanodots in the in-plane FM state (transient state) at the critical magnitude $B_x = B_{c,x}$ of the external bias magnetic field; (b) path of the spectrum plot in (a) (shown by green arrows) and the first Brillouin zone of the array lattice (shown by a gray dashed line). Parameters of the dot array: dot aspect ratio $h/R = 5$, lattice constant $a = 4R$.

note that wave vectors $\boldsymbol{\kappa}$ do not necessarily correspond to a true ground state of the array, as it is, for instance, for a hexagonal array of dots with perpendicular anisotropy.[25,26]

At the critical magnitude of the external bias field, the SW frequency at the point $\boldsymbol{\kappa}$ is zero. If the external field is slightly smaller than critical, the SWs in the vicinity of $\boldsymbol{\kappa}$ become unstable and start to grow exponentially from a thermal level. At the beginning of this process, the amplitudes of the unstable SWs are relatively small and, therefore, the different SWs do not interact with each other (the only exception are the waves with wave vectors $\boldsymbol{k}$ and $-\boldsymbol{k}$, see following). In particular, this means that, at least at the beginning stage of the SW instability, the growing unstable SWs do not suppress the growth of other SWs that have just become unstable.

When the unstable SWs have grown to a sufficiently large level, the nonlinear interaction between them becomes significant. We assume that at this stage the new unstable SWs can not start to grow anymore. This can be easily understood by recalling that the length of the magnetization vector remains constant and, therefore, the z component of the total magnetization is also finite: $M_z \leqslant M_s$. Thus, when the M_z due to the growth of the SW instability reaches the value $M_z \sim M_s$, new unstable SWs can start to grow only due to the nonlinear interaction with already existing unstable SWs. Such a situation, when one SW mode with a small initial amplitude suppresses the SW mode with a large amplitude, requires strong nonlinear interaction and a large difference in the growth increments of the two interacting SW modes.[27] The results of our calculations show that this nonlinear mode competition scenario is not realized in the process of switching of a dipolarly coupled array of magnetic dots. Thus, in all the following we assume that the properties of the final state of a remagnetized dot array are determined by the *linear stage* of the SW instability. After the magnetizations of the dots have reached the level $M_z \sim M_s$, the rapid growth of the unstable SWs ends, and the z components of the dots' magnetizations do not change their signs anymore.

B. Characterization of a final state of a dot array

Due to the shape anisotropy of the dots, after the end of the switching in-plane field pulse and the following relaxation process, the magnetizations of all the dots will be parallel to the z axis: $\boldsymbol{M}_j = \mu_j M_s \boldsymbol{e}_z$, $\mu_j = \pm 1$. Here, j is a two-dimensional index describing the dot position in the array. A natural way to describe a disorder of the final state of the array is to calculate the correlation function

$$\mathcal{K}(j - j') \equiv \langle \mu_j \mu_{j'} \rangle, \tag{3.1}$$

where the angular brackets $\langle \ldots \rangle$ denote averaging over all the dots in the array.

Switching of the array into the final CAFM state is a random process since it is affected by thermal fluctuations. Therefore, one can define another averaging procedure: averaging over different possible realizations of the thermal fluctuations. According to the ergodic hypothesis, these averaging procedures are equivalent in the limit of infinitely large arrays and infinite number of fluctuation realizations, respectively.

The correlation function is directly related to the probability $\mathcal{P}(j)$ that two dots (separated by j lattice parameters) have the same directions of magnetizations:

$$\mathcal{P}(j) = \frac{1 + \mathcal{K}(j)}{2}. \tag{3.2}$$

For the ideal periodic CAFM state, $\mathcal{K}_{id}(j) = (-1)^{j_x + j_y}$, while for a totally disordered state, $\mathcal{K}(j) \to 0$ for a large separation j. The width of the correlation function determines the typical cluster size in a final state of the array. Thus, it is possible to introduce a single number $\mathcal{A}$ that characterizes a typical size of a cluster:

$$\mathcal{A} \equiv \sum_j \mathcal{K}_{id}(j)\mathcal{K}(j). \tag{3.3}$$

The number $\mathcal{A}$ has the meaning of a typical number of dots in one cluster, but it is not exactly the averaged cluster size obtained by dividing the total number of dots in an array by a total number of clusters in this array. Nevertheless, $\mathcal{A}$ is a convenient universal characteristic of the order in the final state of the remagnetized array.

C. Relation between correlation function of a final state with small-angle magnetization dynamics

The main assumption that allows us to relate the final demagnetized state of a dot array to the small-angle dynamics of the dot magnetizations in the transient in-plane FM state is the assumption that when the dynamical part of the dot magnetization $m_j(t) \equiv m_{z,j}(t)$ grows to a substantial level ($|m_j| \sim 1$), the z component of the dot magnetization "freezes," and the dot magnetization does not cross the surface $m_j = 0$ anymore. Therefore, the probability $\mathcal{P}(j)$ that two dots situated at a distance of j lattice parameters have the same directions of magnetizations can be calculated at the linear stage of the switching at a time t_*, when $|m_j(t_*)| \sim 1$. It is assumed that after this time the relative direction of the dot magnetizations does not change anymore, and stays the same until the end of the switching process. Therefore, it is assumed that $\mathcal{P}(j)$ is equal to the probability that m_i and m_{i+j} have the same sign:

$$\mathcal{P}(j) = P(m_i m_{i+j} > 0). \tag{3.4}$$

Since m_i and m_{i+j} are driven by white thermal Gaussian noise, at the linear stage of instability growth, they are joint

random Gaussian variables with zero mean values. Their joint probability density function is given by the expression

$$p(m_i,m_{i+j}) = \frac{1}{2\pi\sqrt{\mathcal{M}^2(0)-\mathcal{M}^2(j)}} \times \exp\left[-\frac{(m_i^2+m_{i+j}^2)\mathcal{M}(0)-2m_i m_{i+j}\mathcal{M}(j)}{2[\mathcal{M}^2(0)-\mathcal{M}^2(j)]}\right], \tag{3.5}$$

where the correlation functions are given by $\mathcal{M}(j) \equiv \langle m_i m_{i+j}\rangle$.

Integrating this probability density function over the regions where $m_i m_{i+j} > 0$, we get

$$\mathcal{P}(j) = \iint_{xy>0} p(x,y)dx\,dy = \frac{1}{2} + \frac{\arcsin(\rho_j)}{\pi}, \tag{3.6}$$

where $\rho_j \equiv \mathcal{M}(j)/\mathcal{M}(0)$ is the normalized correlation function at the linear stage of the instability development (small-angle correlation function). Comparing this expression with Eq. (3.2), it is possible to find the relation between the correlation function $\mathcal{K}(j)$ in the final state of the array and the small-angle correlation function ρ_j in the form

$$\mathcal{K}(j) = \frac{2}{\pi}\arcsin(\rho_j). \tag{3.7}$$

Obviously, here small-angle correlation function $\rho(j)$ has to be calculated at the time t_*. Also, since $\mathcal{M}(0,t)$ has the meaning of the squared magnitude of m_j, the condition for the end of the linear stage of the instability development can be formulated as $\mathcal{M}(0,t_*) \sim 1$.

D. Derivation of dynamical equations for the dot magnetization

As it follows from the previous section, to find the correlation function of the dot magnetizations in the a final state of the array it is necessary to know the dynamics of the z component of the dot magnetization at the linear stage of the magnetization switching. It should be noted that for this purpose one *can not* expand the dynamical magnetization of a dot in a series of dots' SW eigenmodes and use the usual equations for the amplitudes of the normal oscillation modes of a dot [similar to Eq. (3.24) in Ref. 12] for the following reasons: (i) the eigenmode structure of a dot is *time dependent* due to the time-dependent external bias field (switching pulse) and (ii) the normal SW modes can not be introduced at the stage when the SW instability is developing. Thus, one needs to start consideration from the very beginning and to use the well-known and general Landau-Lifshitz-Gilbert equation for the dot magnetization:

$$\frac{d\boldsymbol{M}_j}{dt} = -\gamma \boldsymbol{M}_j \times \boldsymbol{B}_{\mathrm{eff},j} - \frac{\gamma\alpha_G}{M_s}\boldsymbol{M}_j \times (\boldsymbol{M}_j \times \boldsymbol{B}_{\mathrm{eff},j}), \tag{3.8}$$

where the effective magnetic field is given by

$$\boldsymbol{B}_{\mathrm{eff},j} = \boldsymbol{B}_e(t) - \mu_0 M_s \sum_{j'} \hat{N}_{jj'}\cdot \boldsymbol{M}_{j'} + \boldsymbol{B}_T(t). \tag{3.9}$$

Here, $\boldsymbol{B}_e(t)$ is the time-dependent external bias magnetic field (switching pulse), $\hat{\boldsymbol{N}}$ is the mutual demagnetization tensor of magnetic dots,[28] and $\boldsymbol{B}_T(t)$ is the vectorial isotropic Gaussian white noise with zero mean value $\langle \boldsymbol{B}_T\rangle = 0$ and correlation[29]

$$\langle \boldsymbol{B}_T(t)\cdot\boldsymbol{B}_T(\tau)\rangle = \nu^2\delta(t-\tau), \quad \nu^2 = \frac{2\alpha_G kT}{\gamma M_s V}. \tag{3.10}$$

Next, we represent the dot magnetization $\boldsymbol{M}_j$ as a sum of the transient state in-plane magnetization $\boldsymbol{\mu}$ and a small dynamical part of the dot magnetization $\boldsymbol{m}_j$:

$$\boldsymbol{M}_j(t) = M_s[\boldsymbol{\mu} + \boldsymbol{m}_j(t)]. \tag{3.11}$$

The dynamical part of the dot magnetization can be expanded in a series of collective SW modes c_k of the array

$$\boldsymbol{m}_j = \sum_{\boldsymbol{k}}(\boldsymbol{m}_{\boldsymbol{k}} e^{i\boldsymbol{k}\cdot\boldsymbol{r}_j}c_{\boldsymbol{k}} + \text{c.c.}), \tag{3.12}$$

where c.c. denotes complex conjugation. Here, the vector amplitudes $\boldsymbol{m}_{\boldsymbol{k}}$ form an arbitrary fixed basis that can be $\boldsymbol{k}$ dependent or not. The only requirement for choosing the vector amplitudes in this basis $\boldsymbol{m}_{\boldsymbol{k}}$ is the condition that this basis is full or, in other words, that its norm[12] is nonzero $i\boldsymbol{m}^*\cdot\boldsymbol{\mu}\times\boldsymbol{m} \neq 0$. In our particular case, it is convenient to use a circularly polarized basis $\boldsymbol{m} = (0,-i,1)/\sqrt{2}$.

Using this representation, the above-introduced correlation function $\mathcal{M}(j)$ is expressed as

$$\mathcal{M}(j) = \mathrm{Re}\left[\sum_{\boldsymbol{k}}(\langle c_{\boldsymbol{k}}c_{\boldsymbol{k}}^*\rangle + \langle c_{\boldsymbol{k}}c_{-\boldsymbol{k}}\rangle)e^{i\boldsymbol{k}\cdot\boldsymbol{r}_j}\right]. \tag{3.13}$$

Substituting Eqs. (3.11) and (3.12) for the dot magnetization vector in Eq. (3.8) and keeping only the terms linear in $c_{\boldsymbol{k}}$, one can obtain the following equation for the amplitudes c_k of the collective SW modes in the array:

$$\frac{dc_{\boldsymbol{k}}}{dt} = -i\Omega_{\boldsymbol{k}}c_{\boldsymbol{k}} - iS_{\boldsymbol{k}}c_{-\boldsymbol{k}}^* - \Gamma_{\boldsymbol{k}}c_{\boldsymbol{k}} + \eta_{\boldsymbol{k}}(t). \tag{3.14}$$

The coefficients in the above equation are

$$\Omega_{\boldsymbol{k}} = \gamma B + \omega_M\frac{F_{\boldsymbol{\kappa}}^{yy}+F_{\boldsymbol{\kappa}}^{zz}}{2}, \tag{3.15a}$$

$$S_{\boldsymbol{k}} = \omega_M(1+i\alpha_G)\frac{F_{\boldsymbol{\kappa}}^{zz}-F_{\boldsymbol{\kappa}}^{yy}}{2}, \tag{3.15b}$$

$$\Gamma_{\boldsymbol{k}} = \alpha_G\Omega_{\boldsymbol{k}}, \tag{3.15c}$$

where $\omega_M = \gamma\mu_0 M_s$ and the scalar static internal field is given by

$$B = B_{e,x}(t) - \mu_0 M_s F_{\boldsymbol{0}}^{xx}. \tag{3.15d}$$

The thermal fluctuations acting on the collective mode $c_{\boldsymbol{k}}$ are described by the following term:

$$\eta_{\boldsymbol{k}} = \frac{i\gamma\boldsymbol{m}^*\cdot\sum_j \boldsymbol{B}_{T,j}e^{-i\boldsymbol{k}\cdot\boldsymbol{r}_j}}{N_d}, \tag{3.16}$$

where N_d is a number of dots in an array. Noting that the fluctuation field $\boldsymbol{B}_{T,j}$ acting on any particular dot is not correlated with the similar field acting on any other dot and using the statistical properties of the fluctuations (3.10), one can prove that $\eta_{\boldsymbol{k}}$ is a scalar Gaussian delta-correlated

stochastic process with zero mean value and a correlation function given by

$$\langle \eta_{\boldsymbol{k}}(t)\eta^*_{\boldsymbol{k}'}(t')\rangle = \sigma_\eta^2 \delta(t-t')\delta_{\boldsymbol{k},\boldsymbol{k}'}, \tag{3.17a}$$

$$\sigma_\eta^2 = \frac{\gamma^2\nu^2}{3N_d}. \tag{3.17b}$$

Note also, that due to a particular choice of the basis $\boldsymbol{m}$, the processes $\eta_{\boldsymbol{k}}$ and $\eta_{\boldsymbol{k}'}$ are not correlated for any values of the wave vectors.

E. Dynamics of unstable collective SW modes

The dynamics of unstable collective SW modes in the dot array is described by two coupled equations (3.14). The main difficulty in the solution of these equations is the time dependence of their coefficients $\Omega_{\boldsymbol{k}}$ and $\Gamma_{\boldsymbol{k}}$ due to the time-dependent external field magnetic field (switching pulse). It may happen that for a particular choice of the time dependence of the switching pulse $B_e(t)$ it would become possible to find the exact solution of the equations (3.14) analytically. We, however, will concentrate below on the approximate solution of Eqs. (3.14), assuming slow and monotonic time dependence of the field $B_e(t)$ in comparison with the typical period of collective eigenoscillations of magnetization in the array.

The system of equations (3.14) can be reduced to a single inhomogeneous differential equation of the second order

$$\ddot{c}_{\boldsymbol{k}} + 2\Gamma_{\boldsymbol{k}}\dot{c}_{\boldsymbol{k}} + \left(\Omega_{\boldsymbol{k}}^2 - |S_{\boldsymbol{k}}|^2 + i\dot{\Omega}_{\boldsymbol{k}} + \dot{\Gamma}_{\boldsymbol{k}} + \Gamma_{\boldsymbol{k}}^2\right) c_{\boldsymbol{k}} = f(t), \tag{3.18}$$

where $\dot{c} \equiv dc/dt$ denotes the time derivative and the external force $f(t)$ is given by

$$f(t) = \dot{\eta}_{\boldsymbol{k}}(t) - iS_{\boldsymbol{k}}\eta^*_{-\boldsymbol{k}}(t) - i\Omega_{\boldsymbol{k}}\eta_{\boldsymbol{k}}(t). \tag{3.19}$$

One can also obtain a similar equation for $c^*_{-\boldsymbol{k}}$. The solution of the inhomogeneous equation (3.18) with natural initial conditions $c_{\boldsymbol{k}}(t\to-\infty)=0$, $\dot{c}_{\boldsymbol{k}}(t\to-\infty)=0$ can be represented via two linearly independent solutions $x(t)$ and $y(t)$ of a corresponding homogeneous equation as follows:

$$c_{\boldsymbol{k}}(t) = x(t)\int_{-\infty}^{t}\frac{1}{W}f(\tau)y(\tau)d\tau - y(t)\int_{-\infty}^{t}\frac{1}{W}f(\tau)x(\tau)d\tau, \tag{3.20}$$

where $W \equiv \dot{x}y - x\dot{y}$ is the Vronsky's determinant of Eq. (3.18). Thus, it is necessary to find a general solution of a *homogeneous* Eq. (3.18) (with zero right-hand-side part).

To find an approximate solution of Eq. (3.18), one can neglect all the small damping terms containing α_G in the circular brackets. Also, if the external time-dependent magnetic field decreases at a sufficiently slow rate, so that $(dB_e/dt)/B \ll \omega_M$, the term $\dot{\Omega}_{\boldsymbol{k}}$ is significant only during a short-time interval near the transition from the stable to unstable regime and, therefore, can be also dropped. Then, introducing the squared free-running SW frequency as $\omega_{\boldsymbol{k}}^2 \equiv \Omega_{\boldsymbol{k}}^2 - |S_{\boldsymbol{k}}|^2$, we can rewrite the homogeneous part of Eq. (3.18) in following form:

$$\ddot{c}_{\boldsymbol{k}} + 2\Gamma_{\boldsymbol{k}}(t)\dot{c}_{\boldsymbol{k}} + \omega_{\boldsymbol{k}}^2(t)c_{\boldsymbol{k}} = 0. \tag{3.21}$$

It should be noted that the derived dynamical equation (3.21) for the amplitudes of collective SW modes of a dot array is rather general and is applicable not only to the particular case of a square array of uniformly magnetized dots considered in this text, but also for the dot arrays of a different geometry. A similar equation will work even in the case when the ground state of the magnetization in a dot is nonuniform, and will, for example, describe the growth of unstable SW modes in the case of switching of the ground state of dots in an array from uniform to vortex.[30] The only change will be in the frequency $\omega_{\boldsymbol{k}}$ of the soft SW mode, the mode with the largest critical field B_c, which becomes unstable first when the external bias magnetic field is gradually reduced.

To solve Eq. (3.21), we need to find approximations for the functions $\omega_{\boldsymbol{k}}^2(t)$ and $\Gamma_{\boldsymbol{k}}(t)$. Let us define the time origin as the moment when the soft SW mode becomes unstable: $\omega_{\boldsymbol{k}}^2(t=0)=0$. A squared frequency of this soft mode is a smooth function of the external magnetic field (see Appendix) and, thus, of time, if the external magnetic field is also a smooth function of time. Thus, the frequency of the soft mode can be expanded in a common Taylor series near the point $t=0$.

It should be noted that there are two possible types of the soft mode instability: an unstable focus instability and a saddle point. For the focus instability, the linear term in the frequency expansion $\omega_{\boldsymbol{k}}^2(t)$ vanishes and the frequency $\omega_{\boldsymbol{k}}^2$ is non-negative at any time. Thus, the unstable mode grows due to "negative damping." This type of instability can occur only in the cases of high symmetry since it requires the equality of $F_{\boldsymbol{\kappa}}^{yy}$ and $F_{\boldsymbol{\kappa}}^{zz}$ [see Eq. (A1)]. A more common case that, in particular, takes place for the geometry of the square dot array considered above is a saddle-point instability, in which $\omega_{\boldsymbol{k}}^2$ changes sign and becomes negative. In the following, we will consider only this case of a saddle-point instability for which the squared frequency of the soft SW mode can be approximated as $\omega_{\boldsymbol{k}}^2 \approx -\xi t$, where

$$\xi \equiv -\left.\frac{d\omega_{\boldsymbol{\kappa}}^2}{dB_e}\right|_{B_c}\cdot\left.\frac{dB_e}{dt}\right|_{B_c}. \tag{3.22}$$

The damping term in Eq. (3.21) is nonzero at the time $t=0$ and is approximated as

$$\Gamma_{\boldsymbol{k}}(t) \approx \alpha_G\Omega_0, \quad \Omega_0 \equiv \Omega_{\boldsymbol{\kappa}}(B_e=B_c) = \omega_M\frac{F_{\boldsymbol{\kappa}}^{yy} - F_{\boldsymbol{\kappa}}^{zz}}{2}. \tag{3.23}$$

Here, we also assume for simplicity that the only difference between the collective SW modes with different wave vectors is the time when the mode becomes unstable when the external bias field is decreasing and, therefore, the coefficients in the approximate Eq. (3.21) are independent of the wave vector $\boldsymbol{k}$.

Under all the above-described assumptions and simplifications, Eq. (3.21) can be rewritten as

$$\ddot{c}_{\boldsymbol{k}} + 2\alpha_G\Omega_0\dot{c}_{\boldsymbol{k}} - \xi t c_{\boldsymbol{k}} = 0. \tag{3.24}$$

Using the method of slowly varying amplitudes, it is possible to obtain a fundamental solution of Eq. (3.24) in the form

$$x(t) = \mathrm{Ai}(\sqrt[3]{\xi}t)e^{-\alpha_G\Omega_0 t}, \quad y(t) = \mathrm{Bi}(\sqrt[3]{\xi}t)e^{-\alpha_G\Omega_0 t}, \tag{3.25}$$

where Ai and Bi are the Airy's functions. In the range of negative times $t<0$, both Airy's functions are oscillating with the time-dependent period.[31] For positive times $t>0$, the function Bi rapidly increases with time, while the function

Ai rapidly decreases to 0. Keeping only the fastest increasing term, the following expression for the amplitude of the unstable soft SW mode can be obtained:

$$c_{\boldsymbol{k}}(t) = \frac{\pi}{\sqrt[3]{\xi}}\mathrm{Bi}(\sqrt[3]{\xi}t)\int_{-\infty}^{t} f(\tau)\mathrm{Ai}(\sqrt[3]{\xi}\tau)e^{\alpha_G\Omega_0\tau}d\tau. \quad (3.26)$$

Here, we have used the well-known expression[31] for the Airy's functions $\dot{\mathrm{B}}\mathrm{i}(t)\mathrm{Ai}(t) - \dot{\mathrm{A}}\mathrm{i}(t)\mathrm{Bi}(t) = 1/\pi$.

Using the explicit expression for the driving force $f(t)$ [Eq. (3.19)] and taking into account the statistical properties of stochastic process $\eta_{\boldsymbol{k}}(t)$ [Eq. (3.17)], one can find the correlation function for the unstable SW mode

$$\langle c_{\boldsymbol{k}}c^*_{\boldsymbol{k}}\rangle + \langle c_{\boldsymbol{k}}c_{-\boldsymbol{k}}\rangle \approx \frac{4\Omega_0^2\sigma_\eta^2}{\xi^{5/6}\sqrt{\alpha_G\Omega_0}}\mathrm{Bi}^2(\sqrt[3]{\xi}t). \quad (3.27)$$

Here, we retained only the largest term in the correlation function, noting that $\Omega_0 \gg \sqrt[3]{\xi}, \alpha_G\Omega_0$ for typical parameters of a magnetic dot array.

In Eq. (3.27), the time t is defined differently for each particular SW mode, so that each mode becomes unstable at $t = 0$. In "real" time, each SW mode becomes unstable at the moment defined from the condition $\omega^2_{\boldsymbol{k}}(t') = 0$. Using the spectral approximation (A2), this instability condition can be transformed to the following expression for the instability moment of each SW mode $t' = w(\Delta\boldsymbol{k})/\xi$. Noting this and changing the summation over the mode wave vectors $\sum_{\boldsymbol{k}}$ to integration $(N_dS_0/4\pi^2)\int d\boldsymbol{k}$ in Eq. (3.13), we get the following expression for the small-angle correlation function:

$$\mathcal{M}(j) = \frac{\Omega_0^2\gamma^2\nu^2S_0}{3\pi^2\xi^{5/6}\sqrt{\alpha_G\Omega_0}}\mathrm{Re}\times\left[e^{i\boldsymbol{\kappa}\cdot\boldsymbol{r}_j}\int_{\xi t>w(\Delta\boldsymbol{k})}\mathrm{Bi}^2 \times(\sqrt[3]{\xi}[t - w(\Delta\boldsymbol{k})/\xi])e^{i\Delta\boldsymbol{k}\cdot\boldsymbol{r}_j}d\Delta\boldsymbol{k}\right], \quad (3.28)$$

where the integration is performed over all the region of unstable SWs having wave vectors $\boldsymbol{k} = \boldsymbol{\kappa} + \Delta\boldsymbol{k}$. Here, S_0 is the area of an elementary cell of the dot array lattice which is equal to $S_0 = a^2$ for a square lattice.

F. Statistics of a final state of a dot array

Using Eq. (3.28), it is possible to evaluate the statistical properties of the final state of a dot array after the application of a switching in-plane magnetic field pulse. The general scheme of the calculation is as follows: (i) find the time moment t_* at which the growth of unstable SW modes stops from the condition $\mathcal{M}(j = 0, t = t_*) = 1$; (ii) calculate the small-angle correlation function $\mathcal{M}(j)$ at the time t_*; (iii) calculate the correlation function of a final state of the dot array using Eq. (3.7). Knowing the correlation function $\mathcal{K}(j)$ and using Eq. (3.3), one can find an average size of the CAFM clusters in the final state of the array and then can evaluate the microwave absorption curve of an array in its final state (see Sec. V).

Equation (3.28) is general and is applicable to a dot array with an arbitrary dispersion relation $\omega^2_{\boldsymbol{k}}|_{B=B_c} \equiv w(\Delta\boldsymbol{k})$, and in particular to the case when there is more than one unstable point $\boldsymbol{\kappa}$ in the Brillouin zone of the array. In a particular case when there is only one unstable point $\boldsymbol{\kappa}$ in the Brillouin zone and when the SW spectrum near this point $\boldsymbol{\kappa}$ is monotonic and isotropic, so that it can be approximated as $w(\Delta\boldsymbol{k}) = (v|\Delta\boldsymbol{k}|)^2$, an explicit expression for the correlation function $\mathcal{K}(j)$ in the final state of the array can be obtained. The square array of cylindrical dots considered above satisfies these conditions.

In the switching process, all the unstable SW modes start to grow from the thermal level, which is very small, and therefore their amplitudes reach the values $\sim$1 when the argument of the Airy's function in Eq. (3.28) is much greater than 1. Thus, for the most of the unstable SW modes in the final state, the relation $t_* \gg v^2\Delta k^2/\xi$ is satisfied, where v is the group velocity and Δk is the wave-number interval of the unstable SW modes. Using the asymptotic behavior of the Airy's function at large values of the argument $\mathrm{Bi}(x) \approx \exp[2x^{3/2}/3]/\sqrt[4]{\pi^2x}$ and expanding its argument in a Taylor series to the accuracy of $O(\Delta k^4)$, it is possible to obtain the following approximate expression for the Airy's function in Eq. (3.28):

$$\mathrm{Bi}^2(\sqrt[3]{\xi}[t - w(\Delta\boldsymbol{k})/\xi]) \approx \frac{1}{\pi\sqrt{t}\xi^{1/6}}e^{\frac{4}{3}\sqrt{\xi}t^{3/2}}e^{-2\sqrt{\frac{t}{\xi}}v^2\Delta k^2}.$$

With this approximation, it is possible to perform integration in Eq. (3.28) extending the integration limits to all the $\boldsymbol{k}$ space, and to obtain an explicit expression for the small-angle correlation function

$$\mathcal{M}(j) = \mathcal{K}_{id}(j)\frac{\gamma^2\nu^2\Omega_0^{3/2}S_0}{6\pi^2v^2t\sqrt{\alpha_G\xi}}\exp\left[\frac{4}{3}\sqrt{\xi}t^{3/2} - \frac{r_j^2}{8v^2\sqrt{t/\xi}}\right]. \quad (3.29)$$

Here, we have used that $\mathcal{K}_{id}(j) \equiv \mathrm{Re}[e^{i\boldsymbol{\kappa}\cdot\boldsymbol{r}_j}] = (-1)^{j_x+j_y}$. Thus, the normalized small-angle correlation $\rho_j \equiv \mathcal{M}(j)/\mathcal{M}(0)$ that, in the end, defines the correlation function of the final state of the array [see Eq. (3.7)] has a usual Gaussian form, but with a time-dependent dispersion

$$\rho_j(t) = \mathcal{K}_{id}(j)e^{-r_j^2/2\sigma_j^2(t)}, \quad \sigma_j^2(t) = 4v^2\sqrt{t/\xi}. \quad (3.30)$$

As one can see, the dispersion σ_j^2 increases with time, which means that the magnetization dynamics becomes more correlated in space.

As it was mentioned above, the growth of the SW instability stops and the z component of magnetization freezes after the dynamic magnetization of the dot reaches a significant level $m_z \sim \sqrt{\mathcal{M}(0)} \sim 1$, which corresponds to the beginning of a nonlinear interaction between the SW modes. An explicit expression for this moment of time t_* can be obtained using a well-known method of successive approximations. In the zeroth approximation order, this time is equal to $t_*^{(0)} \approx \xi^{-1/3}$ that, finally, leads to the expression

$$t_* = \frac{C_t^2}{\sqrt[3]{\xi}}, \quad C_t = \left[\frac{3}{4}\ln\frac{6\pi^2v^2\sqrt{\alpha_G}\xi^{1/6}}{\gamma^2\nu^2\Omega_0^{3/2}S_0}\right]^{1/3}. \quad (3.31)$$

As one can see, the time t_* depends inversely on ξ and, according to Eq. (3.22), it also depends inversely on the slope dB_e/dt. This is an expected result because the faster is the decrease of the external magnetic field, the larger is the increment of the mode growth and, therefore, the faster the mode reaches the nonlinear stage of its growth.

The value of t_* is only weakly dependent on all the parameters of the dot array and/or the parameters of the

switching pulse, except the parameter ξ determined by the rate of decrease of the external bias magnetic field. For typical parameters of an array (see Sec. IV), the constant C_t is of the order of $C_t \sim 1$–2, so for rough estimation of the t_*, averaged cluster size, etc., one can assume that $C_t \approx 1$. We also note that all the above-developed theory is valid only if the processes of SW mode growth are finished before the end of the switching field pulse, so that the time t_* must be smaller than $t_* < 2\gamma\Omega_0 B_c/\xi$, which, in the end, leads to the following approximate condition for the parameter $\xi < \sqrt{2\gamma\Omega_0 B_c}$ determined by the decrease rate of the amplitude of the switching pulse.

Finally, using the above-evaluated value of t_* in Eq. (3.30) and taking into account relation (3.7), one gets the following expression for the correlation function of the final state of the dot array:

$$\mathcal{K}(j) = (-1)^{j_x+j_y}\frac{2}{\pi}\arcsin e^{-r_j^2/2\sigma_j^2}, \quad \sigma_j^2 = \frac{4v^2C_t}{\xi^{2/3}}. \tag{3.32}$$

For small interdot separations r_j the correlation function decreases as $\mathcal{K}(j)/\mathcal{K}_{id}(j) = 1 - \pi r_j/2\sqrt{2}\sigma_j + O(r_j^2)$, while for large interdot separations it behaves like $\mathcal{K}(j)/\mathcal{K}_{id}(j) \sim 2\exp[-r_j^2/2\sigma_j^2]/\pi$.

Using the above expression for the correlation function in the final state of the array in Eq. (3.3) and replacing the summation over j by integration, an explicit expression for the averaged cluster size can be obtained as

$$\mathcal{A} \approx 17.6\frac{v^2C_t}{a^2(\xi)^{2/3}}. \tag{3.33}$$

Similarly to the dependence of the characteristic time of the SW instability growth t_*, the averaged CAFM cluster size strongly depends on the time derivative of the squared SW frequency ξ, and, therefore, on the time rate of decrease of the external switching magnetic field. Another significant parameter determining the cluster size $\mathcal{A}$ is the relative SW group velocity at the point of instability v/a. As it can be seen from Eqs. (3.7) and (3.31), the range of SW modes that become unstable during the switching process is determined from the condition $v\Delta k < \text{const}$. Thus, for larger values of the SW group velocity, the unstable SW modes are located closer to the wave vector of the initial instability κ that, obviously, leads to a more spatially correlated final state of the dot array.

G. Applicability limits of ground-state switching model

The above-developed theory of a ground-state switching of a dot array is valid if the z component of a dot magnetization "freezes" after the end of the linear stage of the SW instability growth (i.e., at times $t > t_*$). Such a case is realized if the energy of thermal fluctuations is insufficient to overcome the energy barrier between the two opposite orientations of magnetization (the magnitude of which is time dependent) and to change the sign of M_z. In the above-presented calculations, we have assumed that the growth of unstable SWs ends after the magnetization reaches the value of $m_z \sim 1$. More rigorously, this condition can be formulated as a condition for m_z to reach its "equilibrium" value at the instant magnitude of the external in-plane bias magnetic field $m_{eq}(B_e)$ (see red dashed line in Fig. 4). This correction is important to consider for the limits of

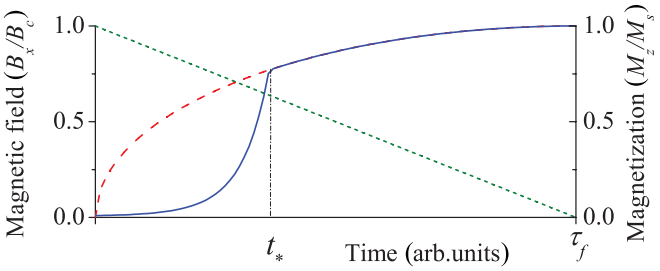

FIG. 4. (Color online) Schematic representation of the magnetization dynamics in a dot array [described by the magnetization vector $M_z(t)$, blue solid line, right axis] during the switching process caused by the application of the in-plane magnetic field $B_x(t)$ (green dotted line, left axis). Red dashed line shows the equilibrium value of the dot magnetization $m_{eq}(B_e)$ at the instant (time-dependent) magnitude of the applied field. Thermal fluctuations of M_z are not shown.

applicability of our model, but does not lead to any qualitative changes in the above-developed theory.

To calculate the equilibrium magnetization $m_{eq}(B_e)$ and the value of the energy barrier, let us assume that the external in-plane magnetic field (directed along the x axis) is smaller than the critical value and that the z components of the dot magnetizations are arranged in an ideal CAFM periodic lattice: $\boldsymbol{M}_j = M_s[\sqrt{1-m_z^2}, 0, (-1)^{j_x+j_y}m_z]$ (which is the most probable state of the dot array). In a Stoner-Wohlfarth model, the value of the energy barrier, which prevents the magnetization from changing the sign of its z component, is determined as a difference between the energy of a particular state and the energy of a state in which the magnetization of only one dot is aligned along the x axis. This energy barrier is equal to

$$\Delta W(t) = \tfrac{1}{2}m_z^2(t)M_sV\left[\mu_0 M_s\left(N_s^{xx} - F_\kappa^{zz}\right) + B_c - B_e(t)\right], \tag{3.34}$$

while the equilibrium magnetization is $m_z^2 = 1 - [B_e(t)/B_c]^2$. The probability of overcoming this barrier due to the thermal fluctuations is given by the Boltzmann distribution $\exp[-\Delta W/kT]$ and the attempt frequency is of the order of the SW eigenfrequency $|\omega_\kappa(t)|$. If the average number of thermally activated jumps during the time interval $t \in [t^*, B_c/\lambda]$ described by the following integral is small,

$$\int_{t^*}^{B_c/\lambda} |\omega_\kappa(t)| e^{-\Delta W(t)/kT} dt \ll 1, \tag{3.35}$$

the z component of the magnetization freezes after the end of the linear stage of mode growth, and, therefore, the properties of a final state of the array are determined only by the linear growth of SW instability. Using expressions (3.31) and (3.34), this condition can be simplified to the following inequality:

$$\xi \gg \left(\frac{2\gamma B_c\Omega_0}{N_s^{xx} - F_\kappa^{zz}}\frac{kT}{\mu_0 M_s^2 V}\right)^{3/2}. \tag{3.36}$$

As one can see, the limits of the described switching regime are determined not only by the relative intensity of the thermal fluctuations, but also by the time rate of decrease of the applied bias magnetic field. With the decrease of this rate, the probability of a different (thermal) switching regime increases due to a smaller value of the equilibrium magnetization at the end of the SW instability growth. For the typical parameters of

a dot array (see Sec. IV), the length of the trailing front of the applied magnetic field pulse has to be shorter than $\tau_f \ll 1\ \mu$s to satisfy the above condition.

In the regime of thermal switching, an array reaches its final state by a sequence of thermal jumps of magnetization. Our numerical simulations have shown that with the increase of temperature, the final state of the array becomes less regular. Also, if the array moves into the regime of thermal switching, when the duration of the trailing front of the switching pulse decreases, the average CAFM cluster size in the array does not increase anymore and can even decrease. Thus, the maximum cluster size in the final state of the array, which can be achieved by increasing the duration of the trailing front of the switching field pulse, is limited by the possible transition into the regime of thermal switching. In particular, one can not expect switching of a large array, consisting of millions of dots, into a perfect periodic ground state by using longer and longer switching field pulses. Possibly, at a larger time scale (with switching pulse durations in the millisecond–second range), the increase of the pulse duration may lead to a more regular final state of the array since the ideal CAFM state is a true ground state of a coupled dot array. However, the detailed investigation of thermal switching regime is beyond the scope of our present work.

IV. COMPARISON WITH NUMERICAL SIMULATIONS

In order to verify the above-derived analytical results, we simulated numerically the magnetization dynamics of a dot array while switching by an applied in-plane magnetic field pulse. For that purpose, we solved a system of stochastic Landau-Lifshitz equations (3.8) using the numerical midpoint rule technique suggested in Refs. 32 and 33. The shape of a switching magnetic field pulse used in our simulations is shown in Fig. 1(c). This pulse consists of a rectangular part of the duration $\tau_x > \tau_{x,c}$ and overcritical magnitude $B_0 = 1.1B_{c,x}$, and a linearly decreasing part $B_e(t) = B_0(1 - t/\tau_f)$. For such a pulse shape, the time derivative of a squared SW frequency is equal to $\xi = 2\gamma\Omega_0 B_0/\tau_f$. All the results presented in the following were calculated for an array of cylindrical magnetic dots with aspect ratio $h/R = 5$ arranged in square lattice with a period $a = 4R$ [see Fig. 1(a)]. The critical field for this particular geometry is equal to $B_{c,x} = 0.23\,\mu_0 M_s$, the array parameter Ω_0 is $\Omega_0 = 0.156\omega_M$, while the SW group velocity in the transient in-plane FM state near the bottom of spectrum corresponding the the wave number $\boldsymbol{\kappa}$ is $v(\phi_{\boldsymbol{k}}) = 0.03a\omega_M$. The other parameters used in our numerical simulations are Gilbert damping constant $\alpha_G = 0.01$, the amplitude of thermal fluctuations $kT/\mu_0 M_s^2 V_d = 3.2 \times 10^{-4}$ (which corresponds to permalloy dots at room temperature $T = 300$ K having the radius $R = 10$ nm), and the size of the simulated array of $N_d = 40 \times 40$ dots with periodic boundary conditions.

First of all, we did five independent simulations of the switching process in the array and obtained five realizations of the final state of the array after switching. Then, we calculated the correlation function $\mathcal{K}(j)$ for each of the simulated final states and took the average of these results, thus obtaining the averaged correlation function of the final state of the array. This result was compared with the analytical calculation made using Eqs. (3.28) and (3.32). The results of this comparison are presented in Fig. 5 and demonstrate excellent agreement between the analytical and numerical data. A small discrepancy between the theory and the numerical simulation seen at $\tau_f\omega_M = 6000$ is caused by the finite-size effects since in this case a final state has only a few CAFM clusters. Also, one can simulate switching of a large dot array, thus replacing the averaging over the calculation realizations by averaging over a large number of dots. However, in this case the correlation function will be really statistically averaged only for the arguments that are much smaller than the size N_d of the array $|j| \ll \sqrt{N_d}$.

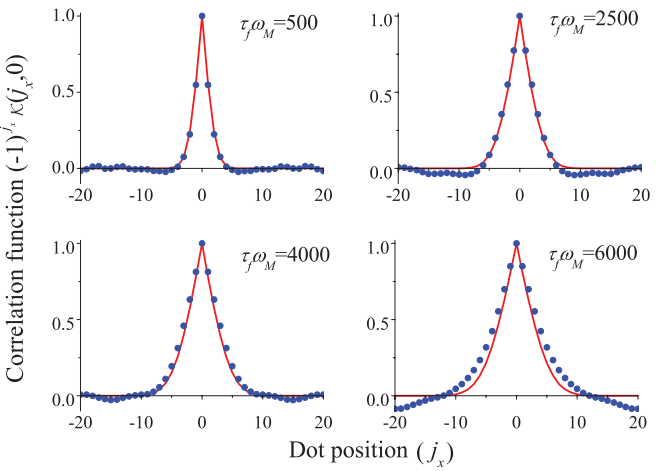

FIG. 5. (Color online) Correlation functions $(-1)^{j_x}\mathcal{K}(j_x, j_y = 0)$ of a final state of a magnetic dot array after the application of a switching field pulse with different durations of the trailing front τ_f. Dots: results of numerical simulations, averaged over five runs; lines: theoretical prediction calculated using Eqs. (3.28) and (3.7).

The calculation of the averaged size $\mathcal{A}$ of a typical CAFM cluster in the final state of the array is especially sensitive to the degree of averaging of the correlation function since the simulated correlation function $\mathcal{K}_{id}(j)\mathcal{K}(j) \equiv |\mathcal{K}(j)|$ for certain realizations can be negative, while the theoretical one and the one that is well statistically averaged are always positive. However, in some cases it is necessary to estimate the cluster size $\mathcal{A}$ from only one particular realization of the final state of the array. In such a case, we propose to use in Eq. (3.3) instead of summation over all the possible j the summation only up to a certain value j', at which $\mathcal{A}(j')$ starts to decrease with the increase of j, thus dropping the negative "tails" of the correlation function modulus. This method is based on the fact that the central part of the correlation function $\mathcal{K}(j)$ (for small values of the correlation function argument) is already well averaged due to a sufficiently large size of the array, while the correlation function of the arguments of the order of array size is substantially influenced by the finite-size effects. We used this method for the calculation of the cluster size $\mathcal{A}$ in the case of large duration of the switching pulse tail, when the array in its final state splits in only a few CAFM clusters.

The dependence of the averaged cluster size $\mathcal{A}$ on field pulse duration is shown in Fig. 6. It is clear from this figure that both full model (3.28) (blue solid line) and the simplified expression (3.33) (red dashed line) demonstrate a reasonably good agreement with the results of numerical calculations (numerical data for $\tau_f\omega_M = 5500$, 6000, from which it seems

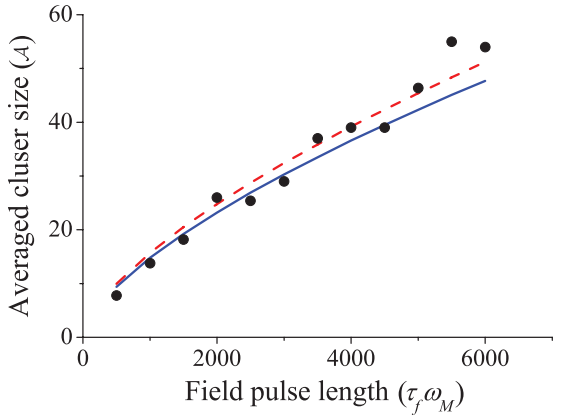

FIG. 6. (Color online) Dependence of the averaged CAFM cluster size $\mathcal{A}$ in the final state of a dot array on the duration of trailing front τ_f of the switching field pulse. Black circles: cluster size $\mathcal{A}$ calculated using, averaged over five realizations, correlation function $\mathcal{K}(j)$ of the numerically simulated final states of the array; lines: theoretical prediction calculated using the full expression (3.28) (blue solid line) and the simplified expression (3.33) (red dashed line).

the simplified expression fits data better may be less accurate since for such values the calculated region divides only on a few clusters). According to the theoretical prediction, the clusters in a final state of the array increase in size as $\mathcal{A} \sim \tau_f^{2/3}$. For all the presented results, the regime with the freezing of the z component of magnetization is realized. According to Eq. (3.36), the transition to the regime of thermal switching starts at $\tau_f\omega_M \gtrsim 10^4$ ($\tau_f \simeq 55$ ns for permalloy). For this value of τ_f, the averaged cluster size is $\mathcal{A} \approx 70$ which is, in fact, close to a maximum cluster size that can be obtained for the array parameters used in our calculations. This cluster size may seem small, but, as it will be shown below, such a quasiregular final state of a dot array has a sufficiently good microwave properties to be useful in practical applications as media with dynamically reconfigurable microwave absorption parameters.

V. MICROWAVE PROPERTIES OF A FINAL STATE

In this section, we discuss the microwave absorption spectra of a magnetic dot array in the final state after the application of a switching magnetic field pulse that leaves the array in a quasiregular CAFM state consisting of several CAFM clusters. We assume that a *spatially uniform* external microwave signal is applied to the dot array and study the absorption of the array as a function of the frequency of the applied microwave signal. In such a case, only quasiuniform spin-wave modes with wave vectors $k \ll \pi/a$ can be excited in the array.

If an array of magnetic dots exists in an ideal periodic ground state, there are several distinct peaks in its microwave absorption spectrum. The number of these peaks is determined by the array's symmetry and, typically, is equal to the number of magnetic sublattices in the array's ground state. The width of each of these absorption peaks, corresponding to different quasiuniform SW modes and having the central frequency ω_p, is determined by the Gilbert damping constant α_G of the dot magnetic material, by the SW mode frequency ω_p, and also by the SW mode ellipticity ε to give $\Delta\omega_p = 2\alpha_G\varepsilon_p\omega_p$.[12] Here, we use a traditional definition of the linewidth $\Delta\omega$ as a full width at half maximum (FWHM).

Any irregularities in the array's periodic ground state lead to the inhomogeneous broadening of the microwave absorption lines. In strongly irregular or disordered ground states, the microwave absorption spectra have a complicated broadened structure that is difficult to describe using the common notions of resonance absorption frequency and FWHM.[16]

However, if a ground state of an array is quasiregular, i.e., consisting of well-defined clusters with ideal periodicity, the microwave absorption spectrum of the array consists of well-defined absorption peaks, the central frequencies of which coincide with the resonance frequencies of the SW modes existing in an ideal periodic demagnetized state (note, however, that if an array in an ideal periodic ground state has a nonzero total magnetic moment, as in the FM state, the absorption peak of the clustered final state will be shifted in comparison with the ideal state due to the different internal magnetic field). The influence of the ground-state irregularity in such a quasiregular array will manifest itself in the changing of the line shape (the line will no longer have a common Lorentzian shape) and in the line broadening (see the inset in Fig. 7). We also note that for a simple square array of identical magnetic dots in the ideal demagnetized (CAFM) state, there is only one microwave absorption peak at the frequency ω_{CAFM} [see Eq. (4.12) in Ref. 12] due to the frequency degeneracy of the collective SW modes, and it is natural and convenient to describe such a simple absorption spectrum using the usual FWHM linewidth.

In general, the shape of a microwave absorption is determined as a convolution of resonance lines caused by the homogeneous damping and inhomogeneous broadening mechanisms.[34] Since different inhomogeneous mechanisms lead to different resonance line shapes, there is no universal relation between the total absorption linewidth and the linewidths caused by each absorption mechanism separately. However, if

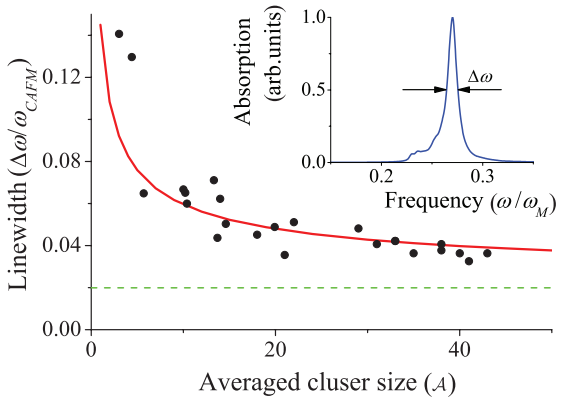

FIG. 7. (Color online) Dependence of the linewidth of microwave absorption in the final state of a remagnetized magnetic dot array on the averaged CAFM cluster size $\mathcal{A}$. Dots: values calculated from the numerically simulated final states of the 24×24 dot array (the method of absorption spectrum calculation described in Ref. 12); solid line: analytical calculation using Eq. (5.1). The microwave absorption linewidth of an array in the ideal periodic CAFM state is shown by a green dashed line. Inset: example of a microwave absorption spectrum of a 24×24 dot array in a final state after the action of a switching field pulse with the trailing front duration $\tau_f\omega_M = 2000$.

both mechanisms lead to the line broadening which is small compared to the resonance absorption frequency, the total FWHM is approximately equal to the sum of the homogeneous and inhomogeneous linewidths $\Delta\omega = 2\alpha_G\omega_{\mathrm{CAFM}} + \Delta\omega_{ih}$.

Obviously, the contribution from the inhomogeneous broadening $\Delta\omega_{ih}$ has to depend inversely on the cluster size in the quasiregular CAFM state. Due to the ground-state irregularity, a spatially uniform microwave field can excite SW modes having nonzero wave vectors. The characteristic values of these wave vectors are of the order of $|\boldsymbol{k}| \sim 1/a\sqrt{\mathcal{A}}$. By fitting the numerical results we have found that the FWHM in a final-state demagnetized state of a magnetic dot array can be approximated by the expression

$$\Delta\omega \approx 2\omega_{\mathrm{CAFM}}\left(\alpha_G + \frac{1}{(a/R)^2\sqrt{\mathcal{A}}}\right). \tag{5.1}$$

The first (homogeneous) term in this expression has been derived in Ref. 12 [see Eq. (3.23) and discussion in Sec. IV B in Ref. 12], while the second (inhomogeneous) term has been obtained empirically by fitting the numerical data. It is clear from Eq. (5.1) that the influence of the inhomogeneous broadening is slowly reduced with the increase of the averaged cluster size $\mathcal{A}$, and also is inversely proportional to the square of the interdot separation a. Obviously, for a sufficiently large separation between the dots, the dipolar coupling between them becomes negligible and all the array's properties are determined by by the magnetic properties of a single dot.

Equation (5.1) gives a reasonably accurate estimation of the FWHM for the magnetic dot arrays in a quasiregular CAFM state at zero permanent field in a wide range of the array's geometrical parameters (see Fig. 7). Obviously, for strongly disordered ground states (for which $\mathcal{A} \lesssim 10$), this estimation is not correct since the microwave absorption line in this case becomes irregular with significant additional absorption lines related to the defect modes (which appear at the border of CAFM clusters). Note that our numerical simulations have shown that the scaling $\Delta\omega_{n/h} \sim 1/\sqrt{\mathcal{A}}$ is rather general and remains the same for other array's geometries (for instance, for nonsquare lattice of the array). However, the coefficient in the term describing the inhomogeneous broadening could be different for different array geometries, in particular for the cases when SW branches are not frequency degenerate at the zero wave vector.

As one can see from Fig. 7, the inhomogeneous broadening becomes smaller than the homogeneous absorption if the average cluster size is about $\mathcal{A} \gtrsim 40$, which makes arrays with this (or larger) cluster size suitable for many practical applications in microwave technology. Note also that in real samples of the magnetic dot arrays there will be an additional mechanism of absorption line broadening related to the imperfections in the geometry of individual dots. Therefore, from the point of view of microwave absorption, the arrays in the ideal CAFM state and in quasiregular states having sufficiently large CAFM clusters will be practically indistinguishable. For our particular square geometry of the array lattice, such quasiregular states can be achieved using field pulses with trailing front duration of the order of $\tau_f\omega_M \gtrsim 4000$ ($\tau_f \simeq 25$ ns for permalloy dots).

VI. SUMMARY

In this work, we developed an analytic theory of ground-state switching in an array of dipolarly coupled magnetic dots. The final ground state of the array is a quasiregular demagnetized state consisting of several reasonably large CAFM clusters. The switching is achieved by application of an in-plane magnetic field pulse with a sufficiently long trailing front. Although the theory was developed for one particular case, i.e., the case of a square array of cylindrical magnetic dots, the developed formalism can be easily adjusted for a dot array having a different geometry. The only geometry-related feature of the considered array of dots is the dispersion relation of the soft collective SW mode in the array.

We have found that the switching process consists of two stages: a relatively short process of growth of unstable SW modes taking place immediately after the transient in-plane FM state of the array becomes unstable, and a relatively slow process of magnetization relaxation to the final demagnetized quasiregular CAFM state, taking place after the SW-related dynamic magnetization reached a sufficiently high level $m \sim 1$. All the properties of the final ground state of the array are determined at the first (short) stage of switching.

The statistical properties of the array's final state are mainly determined by the SW group velocity in the vicinity of bottom (soft) point in the SW spectrum in the transient in-plane FM ground state and by the time derivative of the squared SW frequency, which is directly proportional to the time rate of decrease of the applied switching magnetic field. The final state of the array becomes more regular if the switching field decreases slower. In particular, the averaged size $\mathcal{A}$ of the CAFM clusters in the final state of the array increases as $\mathcal{A} \sim |dB/dt|^{-2/3}$. However, this gradual increase in the regularity of the final array state is limited by the transition into a thermal regime of magnetization switching with the further increase of the switching pulse duration.

The microwave absorption properties of an array in its final demagnetized state are directly related to the statistical properties of the final state of the array. When the final state of the array becomes more regular, the microwave absorption line of the array becomes narrower and approaches the width of the absorption line in the ideal periodic CAFM state as $1/\sqrt{\mathcal{A}}$. The absorption linewidth that is sufficiently narrow for practical applications of the dynamically reconfigurable arrays of magnetic dots in microwave technology is achieved when the switching pulses of a typical duration of 50–100 ns are used.

ACKNOWLEDGMENTS

This work was supported in part by the Grant No. DMR-1015175 from the NSF of the USA, by the contract from the US Army TARDEC, RDECOM, by the DARPA grant "Coherent Information Transduction between Photons, Magnons, and Electric Charge Carriers." K.G. acknowledges support from the IKERBASQUE (the Basque Foundation for Science). The work of R.V., K.G., and G.M. was partially supported by the Spanish MEC Grants No. PIB2010US-00153 and No. FIS2010-20979-C02-01. R.V. and G.M. acknowledge support by MES of Ukraine (Grant No. M/90-2010) and SFFR of Ukraine (Grant No. UU34/008).

APPENDIX

Here, an approximate dispersion relation for the collective spin waves (SW) in a dipolarly coupled array of magnetic dots in a transient in-plane ferromagnetic (FM) state is derived. In general, a dispersion relation for collective SW in a dot array existing in a FM ground state is[12]

$$\omega_{\boldsymbol{k}}^2 = \left[\gamma B_e + \omega_M\left(F_{\boldsymbol{k}}^{yy} - F_{\boldsymbol{0}}^{xx}\right)\right] \times\left[\gamma B_e + \omega_M\left(F_{\boldsymbol{k}}^{zz} - F_{\boldsymbol{0}}^{xx}\right)\right] - \left(\omega_M F_{\boldsymbol{k}}^{yz}\right)^2, \quad \text{(A1)}$$

where the coordinate system is chosen in such a way that the static magnetization of the dot and the external magnetic field are in the x direction. At the critical field $B_c = \mu_0 M_s(F_{\boldsymbol{0}}^{xx} - F_{\boldsymbol{\kappa}}^{zz})$, the frequency at the bottom of the SW spectrum is zero $\omega_{\boldsymbol{\kappa}}(B_c) = 0$. Near these "soft" points one can expand Eq. (A1) in a Taylor series of the form

$$\omega_{\boldsymbol{k}}^2 \approx 2\gamma\Omega_0(B - B_c) + w(\Delta\boldsymbol{k}), \quad \Omega_0 = \omega_M \frac{F_{\boldsymbol{\kappa}}^{yy} - F_{\boldsymbol{\kappa}}^{zz}}{2}. \quad \text{(A2)}$$

Obviously, such an approximation is valid if $\Omega_0 \neq 0$, which corresponds to saddlelike instability.

In any point of the first Brillouin zone aside from the point where $\boldsymbol{\kappa} = \boldsymbol{0}$, the squared SW frequency $\omega_{\boldsymbol{k}}^2$ is a smooth function of the SW wave vector with a minimum at the point $\boldsymbol{\kappa}$. Thus, near this point the squared SW frequency can be expanded as $\omega_{\boldsymbol{k}}^2 \sim (\boldsymbol{k} - \boldsymbol{\kappa})^2$. The case of $\boldsymbol{\kappa} = 0$ is not considered in this work as it corresponds to a trivial switching of the array into a FM state. Finally, we can represent Eq. (A1) for the squared SW frequency in the transitional in-plane ground state in the form

$$\omega_{\boldsymbol{k}}^2 \approx 2\gamma\Omega_0(B - B_c) + [v(\phi_{\boldsymbol{k}})|\Delta\boldsymbol{k}|]^2, \quad \text{(A3)}$$

where $\Delta\boldsymbol{k} = \boldsymbol{k} - \boldsymbol{\kappa}$ and $\phi_{\boldsymbol{k}}$ is the polar angle of the vector $\Delta\boldsymbol{k}$. There is no simple expression for the SW group velocity $\boldsymbol{v}$, so this velocity has to be calculated numerically from the SW spectrum at B_c.

[1] S. Neusser and D. Grundler, Adv. Mater. **21**, 2927 (2009).
[2] A. V. Chumak, A. A. Serga, B. Hillebrands, and M. P. Kostylev, Appl. Phys. Lett. **93**, 022508 (2008).
[3] A. V. Chumak, A. A. Serga, S. Wolff, B. Hillebrands, and M. P. Kostylev, Appl. Phys. Lett. **94**, 172511 (2009).
[4] S. Neusser, B. Botters, and D. Grundler, Phys. Rev. B **78**, 054406 (2008).
[5] V. V. Kruglyak, P. S. Keatley, A. Neudert, R. J. Hicken, J. R. Childress, and J. A. Katine, Phys. Rev. Lett. **104**, 027201 (2010).
[6] A. V. Chumak, V. S. Tiberkevich, A. D. Karenowska, A. A. Serga, J. F. Gregg, A. N. Slavin, and B. Hillebrands, Nat. Commun. **1**, 141 (2010).
[7] J. Jorzick, C. Kramer, S. O. Demokritov, B. Hillebrands, B. Bartenlian, C. Chappert, D. Decanini, F. Rousseaux, E. Cambril, E. Sondergard, M. Bailleul, C. Fermon, and A. N. Slavin, J. Appl. Phys. **89**, 7091 (2001).
[8] Ch. Mathieu, C. Hartmann, M. Bauer, O. Buttner, S. Riedling, B. Roos, S. O. Demokritov, B. Hillebrands, B. Bartenlian, C. Chappert, D. Decanini, F. Rousseaux, E. Cambrill, A. Muller, B. Hoffmann, and U. Hartmann, Appl. Phys. Lett. **70**, 2912 (1997).
[9] J. E. L. Bishop, A. Yu. Galkin, and B. A. Ivanov, Phys. Rev. B **65**, 174403 (2002).
[10] A. Yu. Galkin and B. A. Ivanov, Pis'ma Zh. Éksp. Teor. Fiz., **83**, 450 (2006) [JETP Lett. **83**, 383 (2006)].
[11] P. V. Bondarenko, A. Yu. Galkin, B. A. Ivanov, and C. E. Zaspel, Phys. Rev. B **81**, 224415 (2010).
[12] R. Verba, G. Melkov, V. Tiberkevich, and A. Slavin, Phys. Rev. B **85**, 014427 (2012).
[13] J. Topp, D. Heitmann, M. P. Kostylev, and D. Grundler, Phys. Rev. Lett. **104**, 207205 (2010).
[14] S. Tacchi, M. Madami, G. Gubbiotti, G. Carlotti, S. Goolaup, A. O. Adeyeye, N. Singh, and M. P. Kostylev, Phys. Rev. B **82**, 184408 (2010).
[15] J. C. Slonczewski, J. Magn. Magn. Mater. **159**, L1 (1996).
[16] R. Verba, G. Melkov, V. Tiberkevich, and A. Slavin, Appl. Phys. Lett. **100**, 192412 (2012).
[17] R. Prozorov, Y. Yeshurun, T. Prozorov, and A. Gedanken, Phys. Rev. B **59**, 6956 (1999).
[18] S. I. Denisov and K. N. Trohidou, Phys. Rev. B **64**, 184433 (2001).
[19] S. I. Denisov, T. V. Lyutyy, and K. N. Trohidou, Phys. Rev. B **67**, 014411 (2003).
[20] M. B. Taylor and B. L. Gyorffy, J. Phys.: Condens. Matter **5**, 4527 (1993).
[21] A. B. MacIsaac, J. P. Whitehead, M. C. Robinson, and K. De'Bell, Phys. Rev. B **51**, 16033 (1995).
[22] K. Y. Guslienko, S.-B. Choe, and S.-C. Shin, Appl. Phys. Lett. **76**, 3609 (2000).
[23] E. C. Stoner and E. P. Wohlfarth, Philos. Trans. R. Soc., A **240**, 599 (1948).
[24] *Advanced Magnetic Nanostructures*, edited by D. J. Sellmyer and R. Skomski (Springer, New York, 2006).
[25] R. Verba, Bul. Kyiv Nat. Univ. Radiophys. Electonics **17**, 29 (2012).
[26] A. Joknys and E. E. Tornau, Acta Phys. Polonica A **113**, 951 (2008).
[27] M. I. Rabinovich and D. I. Trubetskov, *Oscillations and Waves in Linear and Nonlinear Systems* (Kluwer, Boston, 1989).
[28] M. Beleggia and M. De Graef, J. Magn. Magn. Mater. **278**, 270 (2004).
[29] G. Bertotti, I. Mayergoyz, and C. Serpico, *Nonlinear Magnetization Dynamics in Nonosystems* (Elsevier, Amsterdam, 2009).
[30] F. G. Aliev, J. F. Sierra, A. A. Awad, G. N. Kakazei, D.-S. Han, S.-K. Kim, V. Metlushko, B. Ilic, and K. Y. Guslienko, Phys. Rev. B **79**, 174433 (2009).
[31] I. S. Gradshteyn and I. M. Ryzhik, *Tables of Integrals, Series and Products*, 7th ed. (Academic, New York, 2007).
[32] M. d'Aquino, C. Serpico, and G. Miano, J. Comput. Phys. **209**, 730 (2005).
[33] M. d'Aquino, C. Serpico, G. Coppola, I. D. Mayergoyz, and G. Bertotti, J. Appl. Phys. **99**, 08B905 (2006).
[34] O. Svelto, *Principles of Lasers* (Plenum, London, 1989).